Journal of Molecular Graphics and Modelling 29 (2010) 256–265

Contents lists available at ScienceDirect

Journal of Molecular Graphics and Modelling

journal homepage: www.elsevier.com/locate/JMGM

Insilico studies on anthrax lethal factor inhibitors: Pharmacophore modeling and virtual screening approaches towards designing of novel inhibitors for a killer

Jyoti Roy, Uday Chandra Kumar, Pavan Kumar Machiraju, Ravi Kumar Muttineni, Suneel Kumar B.V.S*, Rambabu Gundla, Raveendra Dayam, Jagarlapudi A.R.P. Sarma

BioCampus, GVKBIO Sciences Private Limited, S-1, Phase-1, TIE, Balanagar, Hyderabad 500037, AP, India

ARTICLE INFO

Article history:
Received 9 October 2009
Received in revised form 30 June 2010
Accepted 6 July 2010
Available online 15 July 2010

Keywords:
Anthrax
Lethal factor
Pharmacophore
Virtual screening
Bioweapon

ABSTRACT

Bacillus anthracis is a causative organism of anthrax. The main reason to use anthrax as a bioweapon is the combination of the spore's durability and the lethal toxaemia of the vegetative stage. In anthrax infection, lethal factor (LF) is playing crucial role in causing cell death, by inhibiting pathways that rely on this kinase family. The combination of vaccine and antibiotics is preferred as an effective treatment for this target. Till date, no small molecule inhibitor is identified as a drug on the target. In this study, we have performed pharmacophore modeling and docking studies to identify a novel small molecule inhibitor to target the Anthrax LF. The best pharmacophore model is used to screen ~2 M drug-like small molecule database and yielded 2543 hits. Docking studies of the pharmacophore hits on to the active site of Anthrax LF resulted 120 structurally diverse hits. Out of 120 hits, based on synthetic feasibility, 17 hits are selected for further synthesis and pharmacological screening. In due course, we will publish the updated results.

1. Introduction

Bacillus anthracis, the etiological agent of anthrax, has been developed as a bioweapon by countries and terrorists; largely because of the combination of spores durability and lethal toxaemia of the vegetative stage [1]. As a weapon, anthrax is lethal, potent, and highly resistant to sunlight and its stability of anthrax spores in the environment, decontamination requires expensive measures [2]. Anthrax can enter the human body through the intestines (ingestion), lungs (inhalation), and skin (cutaneous) and causes distinct clinical symptoms based on its site of entry. After the toxin enters the human body, the spores germinate into bacteria and secrete a toxin that causes local edema and, in systemic infections, cardiovascular collapse and death [3–5].

The major virulence factor of *B. anthracis* is the anthrax toxin, a tripartite exotoxin comprised of protective antigen (PA, 83 kDa), lethal factor (LF Zn^{2+}, 90 kDa) [EC Number 3.4.24.83], and calmodium-activated edema factor adenylate cyclase (EF, 89 kDa) [6]. The entry of toxin into cells begins with the recognition of a recently identified cellular receptor in the plasma membrane by PA [7]. Proteolytic cleavage of cell-bound PA creates a smaller fragment that then multimerizes into a pore-like structure in the plasma membrane.

The LF and EF proteins bind to the PA pre-pore, followed by internalization of the entire structure through receptor-mediated endocytosis. In the endosomal compartment, the acidic pH causes a conformational change that inserts PA fragments and releases LF and EF into the cytoplasm. In the cytoplasm, edema factor is an adenylate cyclase that inhibits the immune response, including phagocytosis by macrophages. Several potential mechanisms could be used to block anthrax toxin action.

LF acts as a protease that cleaves MAP kinase kinase (MAPKK 1 and MAPKK 2), inhibiting pathways that rely on this kinase family and causing cell death [8]. LF is a Zn^{2+} protease, the only known substrates for which are mitogen-activated protein kinase kinase (MAPKK) isotypes. LF cleaves within the N-terminal proline-rich region that precedes the kinase domain of these proteins, disrupting a protein–protein interaction site involved in assembling signaling complexes, thus preventing MAPKK activation. A structure of LF shows four folding domains. Domain I, which functions in binding to PA63, corresponds to residues 28–263. Domains II–IV is intimately connected with each other and may represent a single folding unit. Domain II has an ADP-ribosyltransferase fold and Domain III is a small helical bundle inserted into Domain II and appears to contain tandem repeats of a structural element of Domain II. Domain IV is distantly related to the thermolysin family of metalloproteases and contains the HEXXH Zn^{2+}-binding motif.

Currently there are only two counter measures available for anthrax: antibiotics and vaccine. Even with successful antibiotic treatment and vaccination, anthrax toxins can remain in the blood

* Corresponding author. Tel.: +91 9849960123.
E-mail addresses: suneel.bommisetty@gvkbio.com, suneelkumar.bvs@gmail.com (S. Kumar B.V.S).

1093-3263/$ – see front matter © 2010 Elsevier Inc. All rights reserved.
doi:10.1016/j.jmgm.2010.07.002

stream and cause lethality. "Our findings make it clear that combination therapy with antibiotics and vaccination is better than either treatment alone," says Douglas Owens, MD, senior investigator at the VA-Palo Alto on anthrax infection and the best strategy is actually the least expensive [9–13].

At present only one vaccine "Anthrax Vaccine Adsorbed (AVA, trade name BioThrax)" is available for anthrax infections and was developed by Emergent BioDefense Corporation. Another vaccine NCT00114621 developed by NICHD is presently in clinical trial phase-1. It was produced by genetic engineered protective antigen (rPA) that brings about antibodies to neutralize the anthrax toxin. Vaccination against anthrax has been confined to people at risk, such as wool sorters and some veterinarians. However, the rising prospects of *B. anthracis* being used as a weapon have led to routine administration of the anthrax vaccine to members of the armed forces.

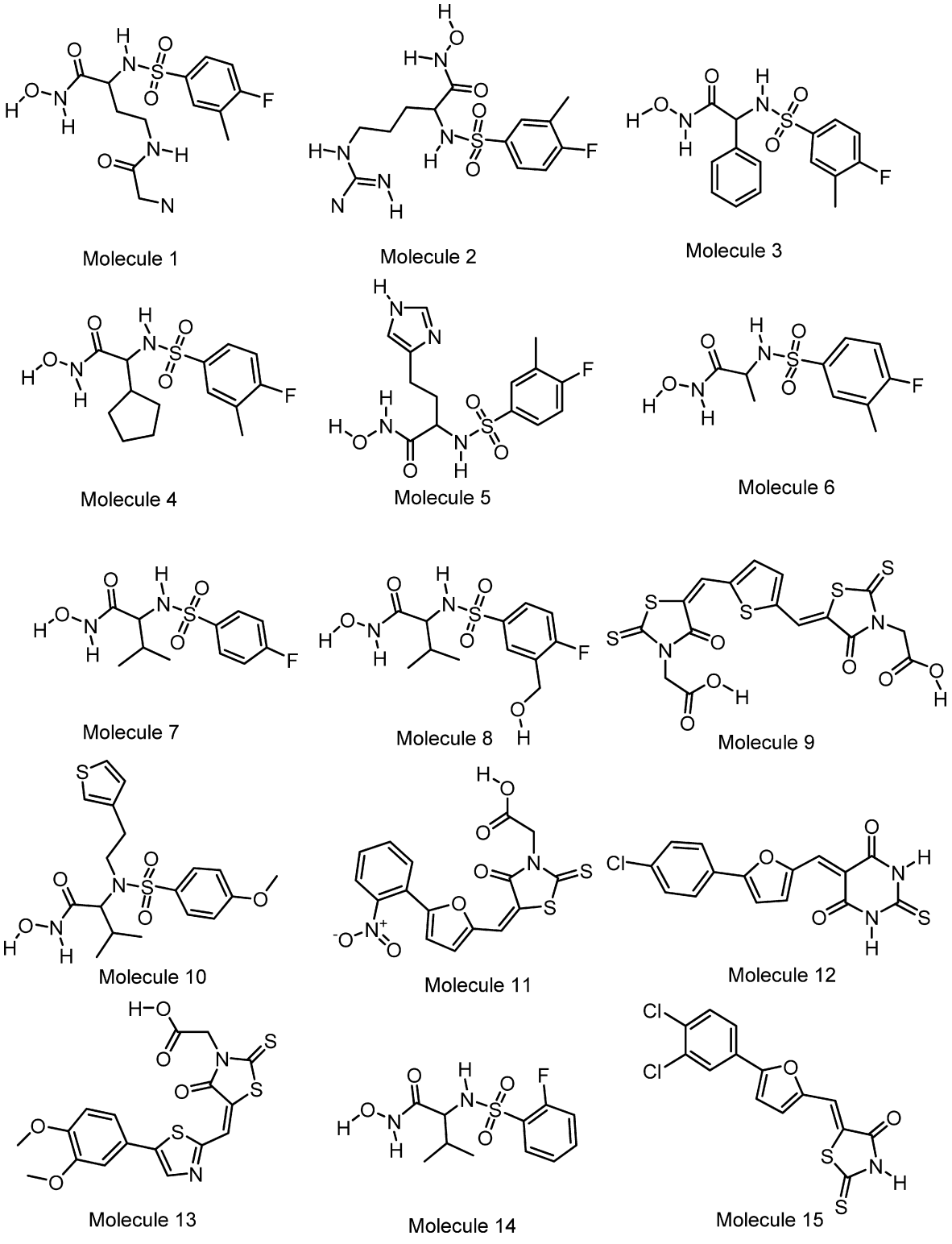

Scheme 1. Chemical structures of the 24 training set molecules applied to HypoGen for pharmacophore generation.

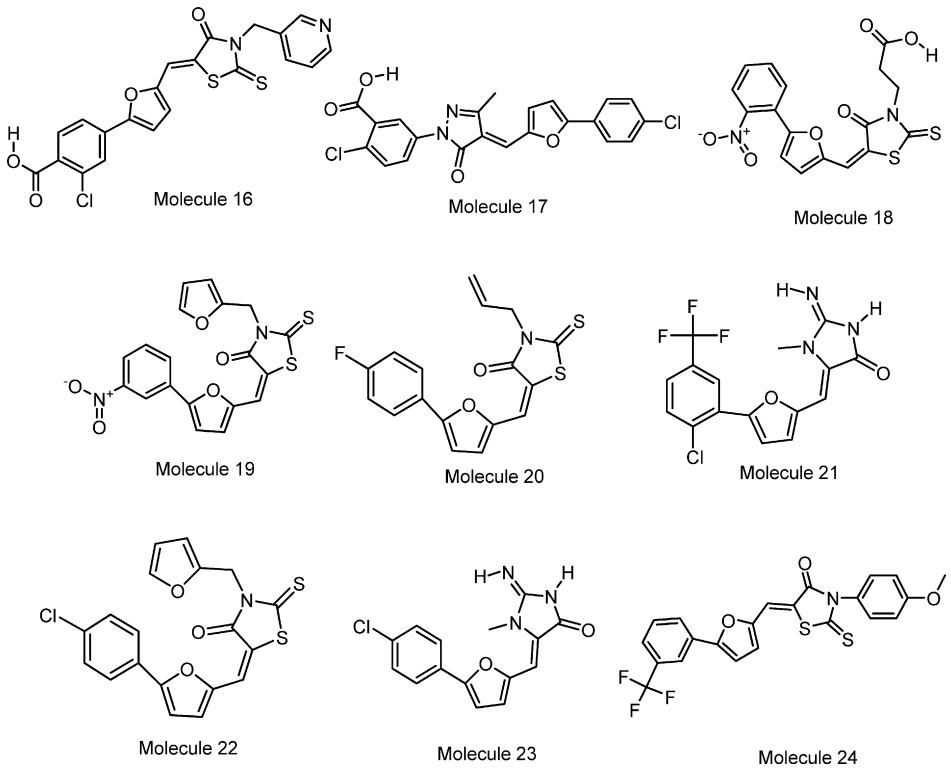

Scheme 1. (*Continued*).

Around 250 small molecules were collected from literature targeting LF activity. However, no inhibitor was translated to clinical phase. The use of computational methods has had a major impact on modern drug design and was firmly recognized as a necessary element of any drug development. In the present study, we developed a pharmacophore model, which provides the key structural features required to design novel Anthrax LF inhibitors. This pharmacophore model was compared with docking interactions and its predictability to accurately estimate activity of known LF inhibitors was ascertained. This validated model was further used for virtual screening.

2. Methodology

2.1. Ligand and protein preparation

In this study, 122 Anthrax LF inhibitors with activity data (IC_{50}) spanning more than four orders of magnitude (from 0.037 μM to 300 μM) [14] collected from literature were considered. The same assay method was used to measure the activity of all the compounds used in this study. The 3D structures of all molecules were constructed using Cerius2 [15] and were subjected to energy minimization using the smart minimizer algorithm with a convergence gradient value of 0.001 kcal/mol. Further geometry optimization was carried out with the MOPAC 6 packages using the semi-empirical AM1 Hamiltonian method [16].

X-ray crystal structure of Anthrax LF (PDB ID 1PWU with a resolution of 2.70 Å) [17] was used in the docking studies. Protein preparation and minimization was performed in InsightII. The active site was visually inspected and the appropriate corrections were made for tautomeric states of histidine residues, orientations of hydroxyl groups and protonation states of basic and acidic residues. The protein with optimized hydrogen positions was finally saved as a separate file to be used for docking. Hydrogen atoms were added to the protein, and the hydrogen atoms were minimized for 5000 steps with steepest decent and followed by conjugate gradient for 3000 steps with all the heavy atoms (non-hydrogen) constrained to their original positions.

2.2. Pharmacophore generation

A pharmacophore model consists of a 3D arrangement of a collection of features necessary for the biological activity of the ligands. The features in catalyst are associated with location constraints, displayed as colored spheres, which allow a certain spherical tolerance surrounding the ideal position of a particular feature in 3D space.

Pharmacophore models were generated for known inhibitors of Anthrax LF using catalyst [18]. Catalyst software allows the generation of pharmacophore models, also termed as hypotheses. In fact, according to Sutter et al. [19] the quality of the pharmacophore model should be as good as the information data input. The most active compounds should inevitably be included in the training set, and all biologically relevant data should be obtained by homogeneous procedures. Taking into account these requirements, we defined a training set of 24 compounds, presented in Scheme 1 and 98 compounds as test set (shown in Supporting information S1).

Conformational models of all the compounds were generated using a Monte Carlo-like algorithm together with poling, to generate a maximum of 250 conformers within the constraint of a 20 kcal/mol energy threshold above the estimated global minimum based on CHARMm force field. Poling is a method for promoting conformational variation that forces similar conformers away from each other. Conclusively, poling improves the coverage of the conformational space [20–22]. The molecules associated with their conformation models were then submitted to catalyst hypotheses generation.

In hypotheses generation, the structure and activity correlations in the training set were rigorously examined. HypoGen identifies features that are common to the active compounds but excludes

Table 1
Results of pharmacophore hypothesis generated using training set against Anthrax LF inhibitors.

Hypo no	Total cost	Cost – difference[a]	Error cost	RMS	Correlation	Features
1	104.00	55.16	91.62	0.95	0.93	A,A,H,H
2	106.17	52.99	94.24	1.06	0.91	A,A,H,H
3	107.17	51.99	95.09	1.09	0.90	A,A,H,H
4	111.95	47.21	99.70	1.25	0.87	A,A,D,H
5	112.58	46.58	100.49	1.28	0.86	A,A,H,H
6	113.43	45.73	101.31	1.30	0.85	A,A,H,H
7	114.24	44.92	101.88	1.32	0.85	A,A,H,H
8	115.29	43.87	102.76	1.35	0.84	A,A,D,H
9	115.54	43.62	103.63	1.13	0.84	A,A,D,H
10	115.88	43.28	103.98	1.39	0.83	A,A,H,H

A = hydrogen bond acceptor, D = hydrogen bond donor, H = hydrophobic.
[a] Cost difference: Null cost – total cost. Fixed cost: 92.62, configuration cost: 10.77 and null cost: 159.16; all cost values are in bits.

common features for the inactive compounds within conformationally allowable regions of space. Ten hypotheses were generated for every HypoGen run from which the ones with the highest correlation values were chosen. The selected pharmacophore model was validated using cost analysis and test set activity prediction. The best pharmacophore (Hypo 1) having highest correlation coefficient (r^2), lowest total cost, and lower RMSD value was chosen to estimate the activity of test set.

2.3. Docking studies

2.3.1. Ligand fit

Using ligand fit, the initial protein-shape-based binding sites were identified using the "site search" module with a value of 9 Å for the site opening [23]. These sites were edited manually with selective additions and deletions in the Cerius2 interface to remove artifacts and to ensure that site points were present around key active site residues. The centroid of the site model was used to define an active site box. Best pose was selected on the basis of dock score and the interactions formed between the ligands and important amino acids.

3. Results and discussion

3.1. Pharmacophore studies

Pharmacophore model of Anthrax LF inhibitors was generated using the HypoGen module in catalyst. HypoGen attempts to construct the simplest hypothesis that best correlates the activities (experimental vs. predicted). The dataset was divided into training set (24 compounds, Scheme 1) and test set (98 compounds in Supporting information S1), considering both structural diversity and wide coverage of the activity range.

At the end of a run, HypoGen returns 10 pharmacophore models. The null cost for 10 hypotheses was 159.16, the fixed cost of the run was 92.62 and the configuration cost was 10.77. A difference of 66.54 bits obtained between fixed and null cost is a sign of highly predictive nature of hypotheses. All 10 hypotheses generated showed high correlation coefficient between experimental and predicted IC_{50} values, in the range of 0.93–0.83; and moreover, these had cost difference greater than 43 bits between the cost of each hypothesis and the null cost. This indicates that all the hypotheses have true correlation between 75% and 90%. The cost values, correlation coefficients (r^2), RMSD, and pharmacophore features are listed in Table 1. The best pharmacophore (Hypo 1) consisted of two H-bond acceptors (HBA) and two hydrophobic (HY) features (shown in Fig. 1) with a correlation coefficient (r^2) of 0.93, total cost (104), and the lowest RMSD value (0.95 Å) was chosen to further validate its predictive power by estimating the activity of test set.

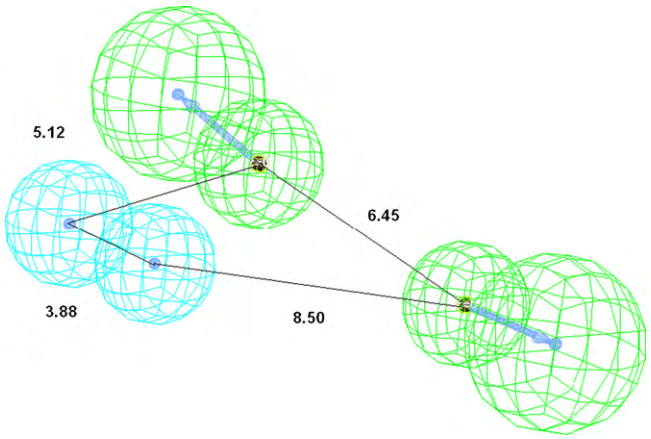

Fig. 1. The best pharmacophore model Hypo 1 produced by the HypoGen module in Catalyst 4.11 software. Pharmacophore features are color-coded with green, cyan contours representing the hydrogen bond acceptor feature (A), hydrophobic feature (Z) respectively. The distances between the features is in Å.

The experimental and predicted Anthrax LF inhibitory activities of the 24 compounds are listed in Table 2. In the training set, all of the features of the Hypo 1 were mapped well to the highly active compounds and it predicts the activity of these compounds correctly. For the least active compounds, the model was able to predict the activity in the same order. At least one feature is missing to map with the least active compounds as the entire feature and their arrangement is important for highly active compounds.

The highest active compound (1) in the training set perfectly mapped all the features of Hypo 1 and had a fit score of 7.64, shown in Fig. 2(a). Whereas, for the least active compound (24), only three features were mapped properly and had a fit value of 4.15, shown in Fig. 2(b).

As depicted from Fig. 2(a), out of the two hydrogen bond acceptor features of the model, HBA1 was mapped to the electron rich oxygen atoms of sulphur dioxide group and HBA2 was

Table 2
Experimental activities and pharmacophore predicted activities of training set molecules.

Molecule number	Experimental activity	Estimated activity
1	0.037	0.046
2	0.04	0.047
3	0.05	0.036
4	0.064	0.25
5	0.075	0.047
6	0.13	0.15
7	0.29	0.34
8	0.6	0.51
9	1.6	4.1
10	2.1	4.2
11	3.1	3.2
12	4.4	23
13	5	4.8
14	6.6	10
15	7.4	25
16	9.9	16
17	11	9.3
18	13	2.4
19	37	8.1
20	50	150
21	100	13
22	150	44
23	200	170
24	300	140

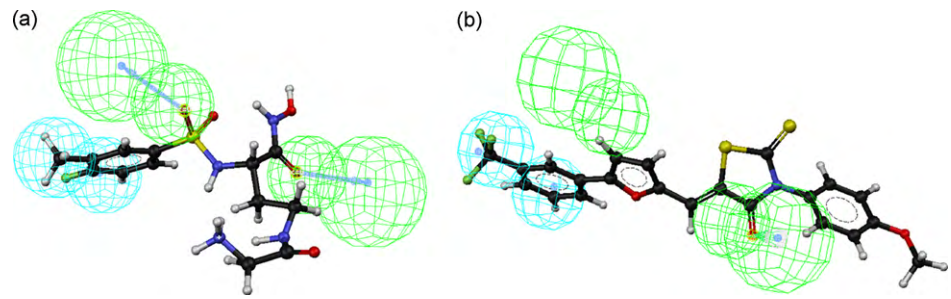

Fig. 2. Pharmacophore mapping of the most active and least active compound (from the training set) on the best hypothesis model Hypo 1 (a). Pharmacophore mapping of the highest active compound 1 from the training set on the best hypothesis model Hypo 1. (b) Pharmacophore mapping of the least active compound 24 on the best hypothesis model Hypo 1.

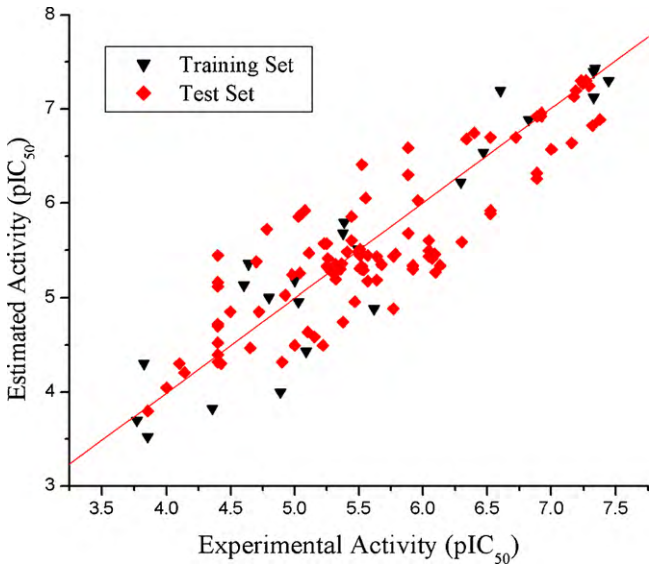

Fig. 3. Correlation graph between experimental and Hypo 1-estimated activities of training and test set.

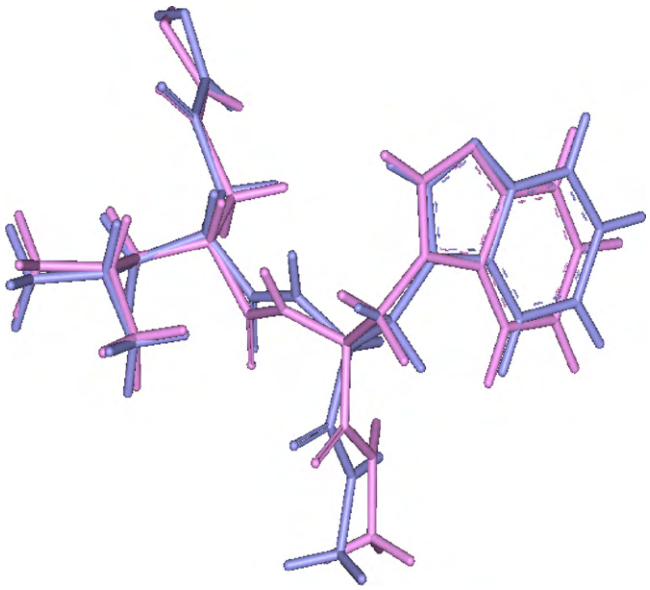

Fig. 5. Superimposition of crystal ligand of 1PWU and redocked pose of crystal ligand generated using LigandFit. Crystal conformation has shown in violet color and redocked conformation in pink color (For interpretation of the references to color in this figure legend, the reader is referred to the web version of this article.).

mapped to the electron rich carbonyl oxygen of hydroxamic acid. The hydrophobic groups were mapped to the benzene ring and methyl group attached at the meta-position of the benzene ring.

The predictability of Hypo 1 was evaluated using a diverse test set compounds. The Hypo 1 pharmacophore model predicted the activity of the 98 test set compounds with a correlation coefficient (r^2) of 0.774 (Fig. 3). Pharmacophore mapping of the highest active compound in the test set is shown in Fig. 4(a) and mapping of the least active compound of the test set is shown in Fig. 4(b). The predicted activities of the compounds along with the scale were listed in the Table 3 .

3.2. Docking studies

Docking studies were performed for 122 small molecule LF inhibitors with the solved 3D-structure of Anthrax LF (PDB entry code 1PWU, 2.70 Å), using ligand fit module in Cerius2. The reliability of this docking method to predict the bioactive conformation was validated using the X-ray structure of Anthrax LF in complex with a co-crystal molecule (3-N-hydroxycarboxamido)-2-isobutylpropanoyl-trp-methylamide (GM6). Co-crystal GM6 was re-docked into the active site of Anthrax LF and the best-docked conformation having lowest docking energy was selected as the

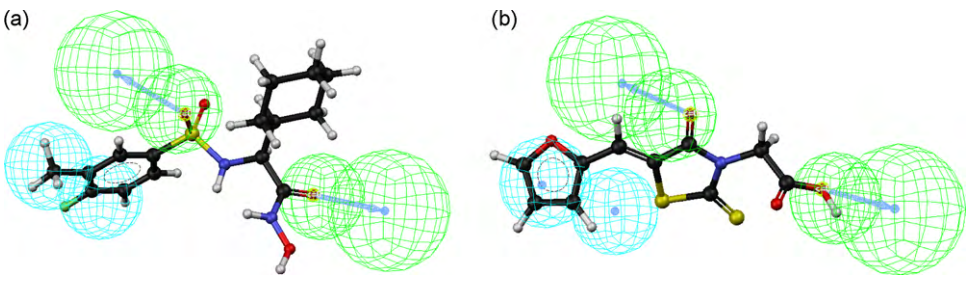

Fig. 4. Pharmacophore mapping of the most active and least compounds from the test set on the best hypothesis model Hypo 1. (a) Pharmacophore mapping of the highest active compound 25 on the best hypothesis model Hypo 1. (b) Pharmacophore mapping of the least active compound 122 on the best hypothesis model Hypo 1.

Table 3
Experimental activities and pharmacophore predicted activities of test set.

Compound number	Experimental activity	Estimated activity
25	0.042	0.13
26	0.048	0.15
27	0.051	0.057
28	0.054	0.05
29	0.057	0.054
30	0.059	0.05
31	0.065	0.064
32	0.067	0.074
33	0.07	0.23
34	0.1	0.27
35	0.12	0.11
36	0.12	0.12
37	0.13	0.12
38	0.13	0.48
39	0.13	0.55
40	0.19	0.2
41	0.26	0.2
42	0.298	1.2
43	0.3	0.2
44	0.4	0.18
45	0.46	0.21
46	0.5	2.6
47	0.74	4.6
48	0.8	5.4
49	0.81	3.5
50	0.85	3.9
51	0.9	3.2
52	0.9	2.5
53	1.1	0.94
54	1.2	5
55	1.2	4.6
56	1.3	2.1
57	1.31	0.5
58	1.31	0.26
59	1.64	3.5
60	1.7	3.7
61	1.7	13
62	2.1	4.5
63	2.3	3.7
64	2.3	6.5
65	2.7	3.6
66	2.7	6.7
67	2.8	0.89
68	2.9	5.1
69	3	4.7
70	3	5
71	3	0.39
72	3.1	3.1
73	3.1	4.9
74	3.1	3.3
75	3.2	3.3
76	3.4	11
77	3.6	2.5
78	3.6	1.4
79	3.9	3.3
80	4.2	18
81	4.3	4.4
82	4.4	5
83	4.4	5
84	4.78	6.4
85	4.8	5.4
86	4.8	4.5
87	5.18	5.3
88	5.5	3.9
89	5.6	2.7
90	5.9	2.7
91	6	32
92	7	26
93	7.7	3.4
94	7.9	23
95	8.3	1.2
96	9.1	5.5
97	9.3	1.4
98	10	32
99	10.5	5.7
100	11.88	9.4
101	12.6	48
102	15	13
103	15	13
104	16.6	1.9
105	19.1	14
106	20	4.2
107	22.4	34
108	31.9	14
109	37.7	50
110	40	40
111	40	48
112	40	3.6
113	40	7.6
114	40	20
115	40	6.9
116	40	19
117	40	30
118	42	40
119	72.4	62
120	79.4	50
121	100	90
122	140	160

most probable binding conformation. The superimposition of the ligand fit docked pose of GM6 with the co-crystal of 1PWU is shown in Fig. 5. The root mean-square deviation (RMSD) between these two poses is 1.10 Å, indicating a high docking reliability of ligand fit in terms of reproducing the experimentally observed binding mode for Anthrax LF inhibitors.

The entire set of 122 inhibitors was docked into the active site of Anthrax LF and the correlation was calculated between dock score and the IC_{50} by linear regression analysis method. An acceptable correlation coefficient (r^2) of 0.803 was obtained between experimental IC_{50} and docking energy (Fig. 6). This correlation strongly indicates that the binding conformations and binding models of the LF inhibitors of Anthrax LF are reliable.

As shown in the Fig. 7(a and b), the best-docked conformation the most active compound (1) forms important hydrogen bond interactions. The first hydrogen bond is formed between the oxygen group of sulphone in compound 1 and with the main chain amine group of Lys656 (O–HN, 2.70 Å). The second hydrogen bond interaction is observed between the carbonyl oxygen of the hydroxamic acid of the compound with the side chain hydroxyl group of Tyr728

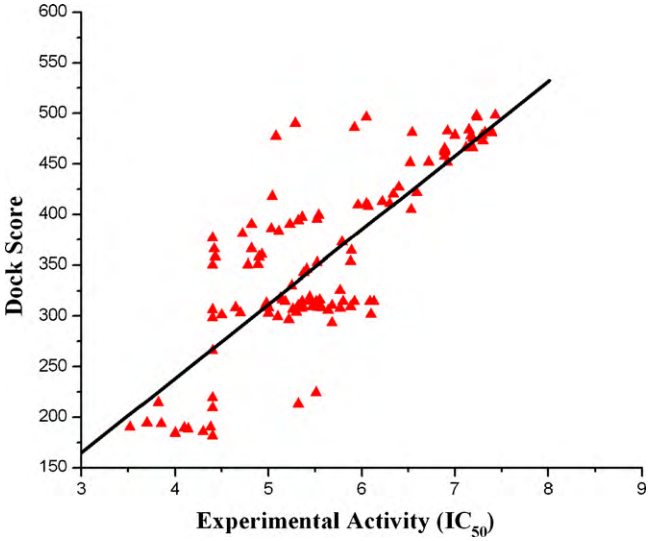

Fig. 6. Graphical representation of correlation between dock score and experimental activity of LF inhibitors.

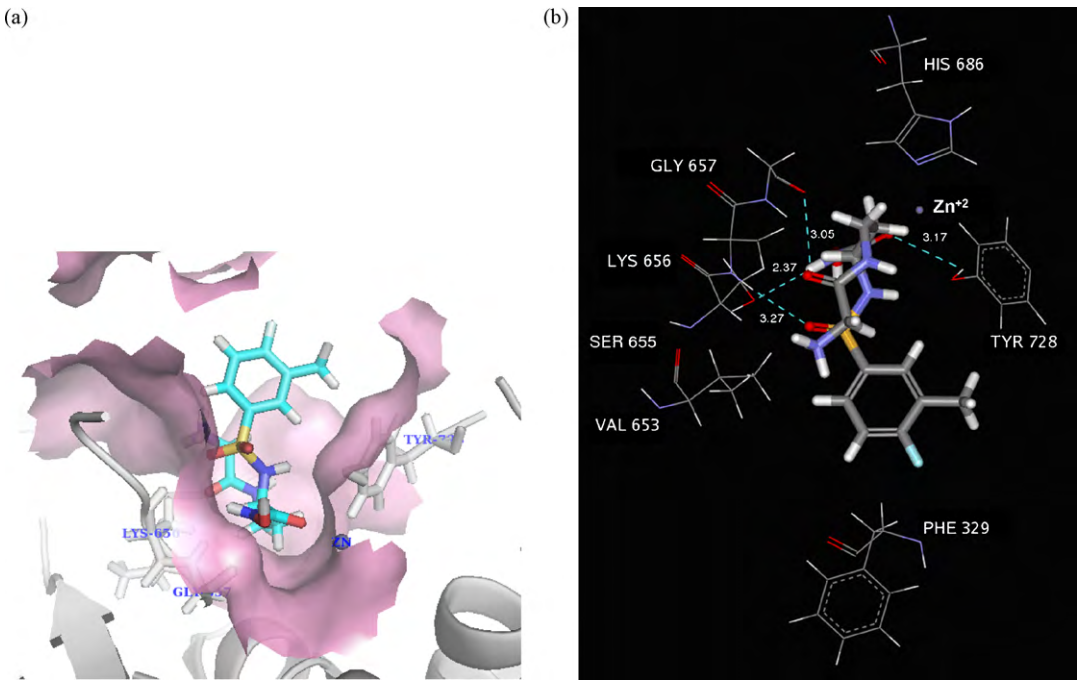

Fig. 7. (a) Docked conformation of the most active (1) in the active sites of 1PWU. (b) Representation of interaction between the docked conformation of the compound 1 in the active sites of 1PWU. Dashed lines represent hydrogen bonds.

(O–HO, 3.12 Å). The third hydrogen bond interactions are observed between the amine group of hydroxamic acid and hydroxyl group of Ser655 (NH–O, 2.24 Å). Other atoms of the compound are also involved in hydrogen bonding, enhancing its binding in the active site. The zinc ion has strong electrostatic interactions with the surrounding amino acids (Tyr728) and the hydroxamic acid group of the compound. The benzene ring and the methyl group present at the meta-position are located in the hydrophobic pocket formed by amino acids: Phe329, Val653 and Val675.

The best-docked pose of least active molecule (24) forms only two interactions with amino acids of the active site (Fig. 8(a and b)). The first hydrogen bond is formed between the carboxyl group attached at the 4th position of 2-thioxo-thiazolidine with the side chain hydroxyl group of Tyr728 (O–HO, 3.21 Å). The second hydrogen bond is formed between the electron rich oxygen group of the furan ring attached to the 5th position of 2-thioxo-thiazolidin and the main chain amine group of Lys656 (O–HN, 2.90 Å). The benzene ring and tri-fluoro methyl

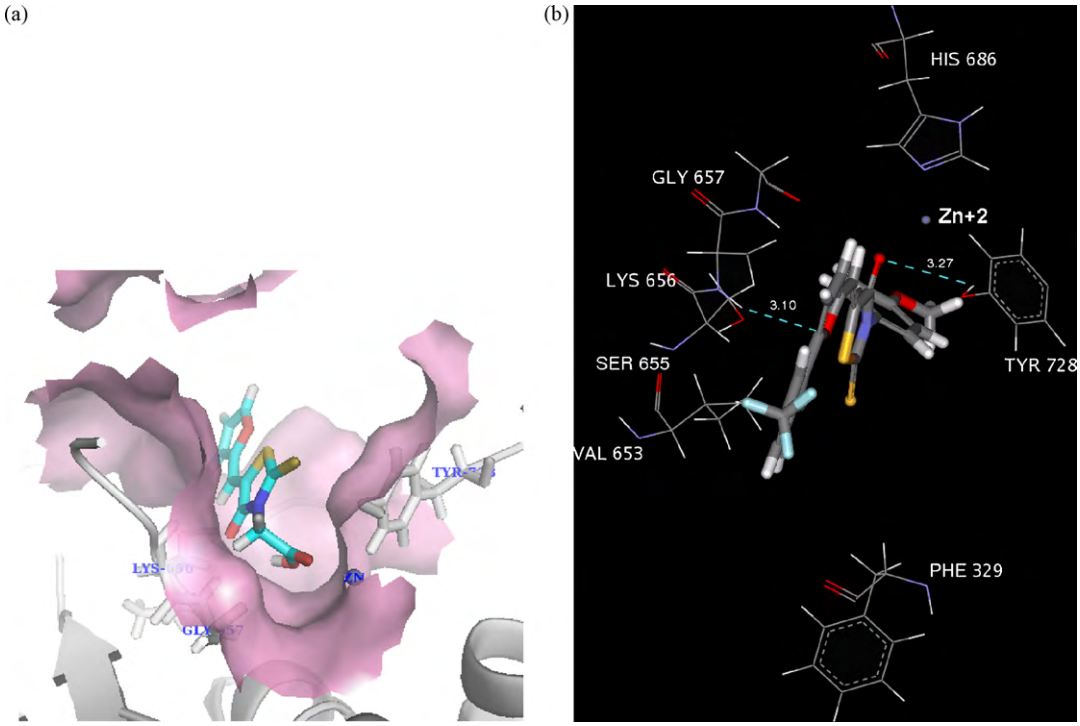

Fig. 8. (a) Docked conformation of the least active compound 122 in the active site of 1PWU. (b) Representation of interaction between the docked conformation of the least active compound 122 in the active sites of 1PWU. Dashed lines represent hydrogen bonds.

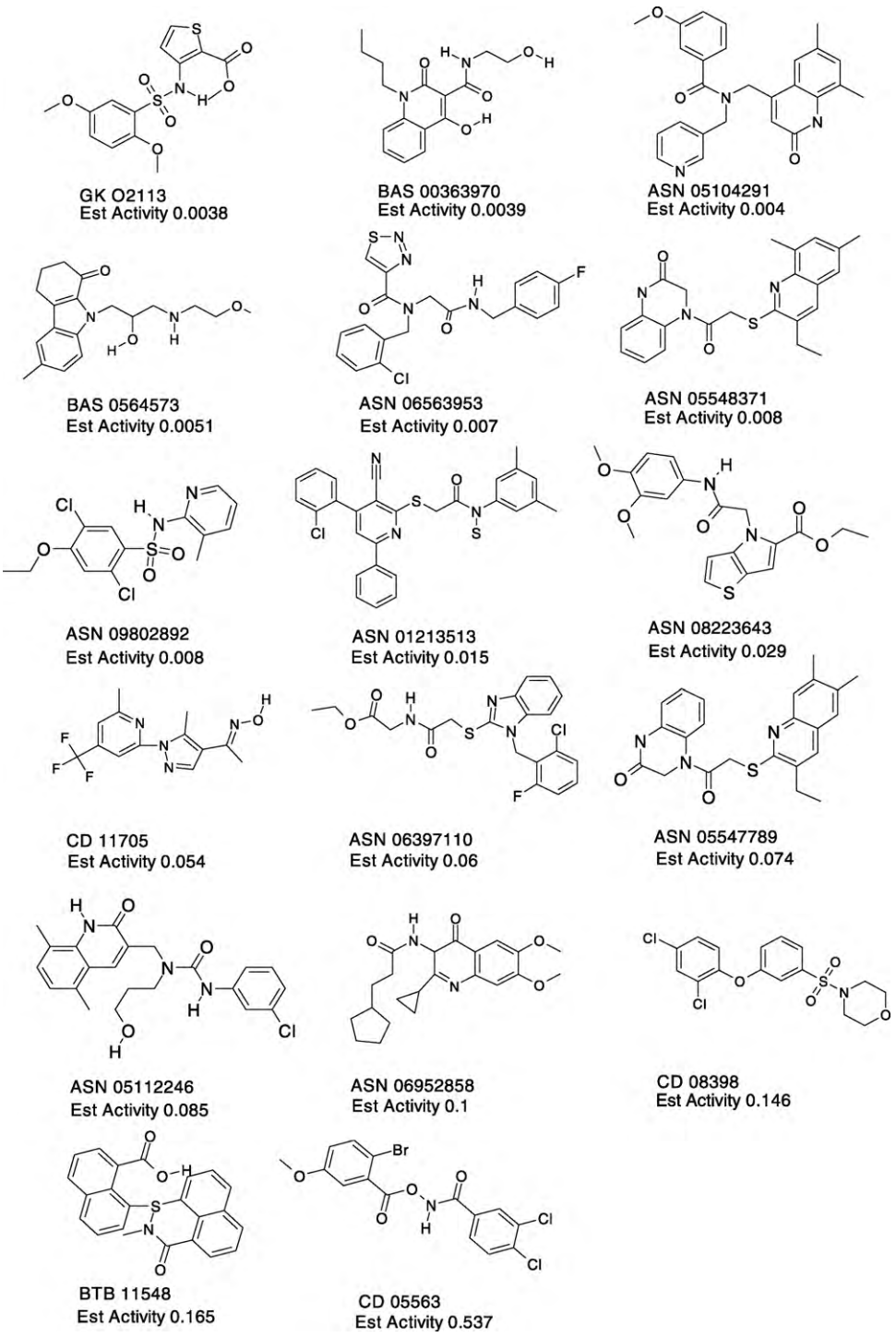

Scheme 2. 2D structures of the virtual screening molecules (estimated activity μM).

attached to its meta-position are positioned in the hydrophobic pocket.

3.3. Comparison of pharmacophore and docking interactions

The obtained pharmacophore model (Hypo 1) correlates very well with the docking interactions (Fig. 7(b)). As shown in Fig. 2(a), the two HBA features (HBA1 and HBA2) are mapped to oxygen moieties of sulphone and the carbonyl group of hydroxamic acid group, thus complementing the hydrogen bond interactions with Lys656 and Tyr728 in the docked pose. Two hydrophobic features map the benzene ring and the methyl moiety attached to its meta-position respectively, and the best-docked pose also depicts the same interaction. The hydrophobic pocket amino acids Phe329, Val653 and Val67. The best pharmacophore model (Hypo 1) mimics the active site interactions and is able to reproduce the important features needed for binding and is very well able explore the docking interactions.

4. Virtual screening

The best pharmacophore model (Hypo 1) was used as a virtual screening query, to identify novel and potent candidates for biological testing if it can identify potential compounds that satisfy the

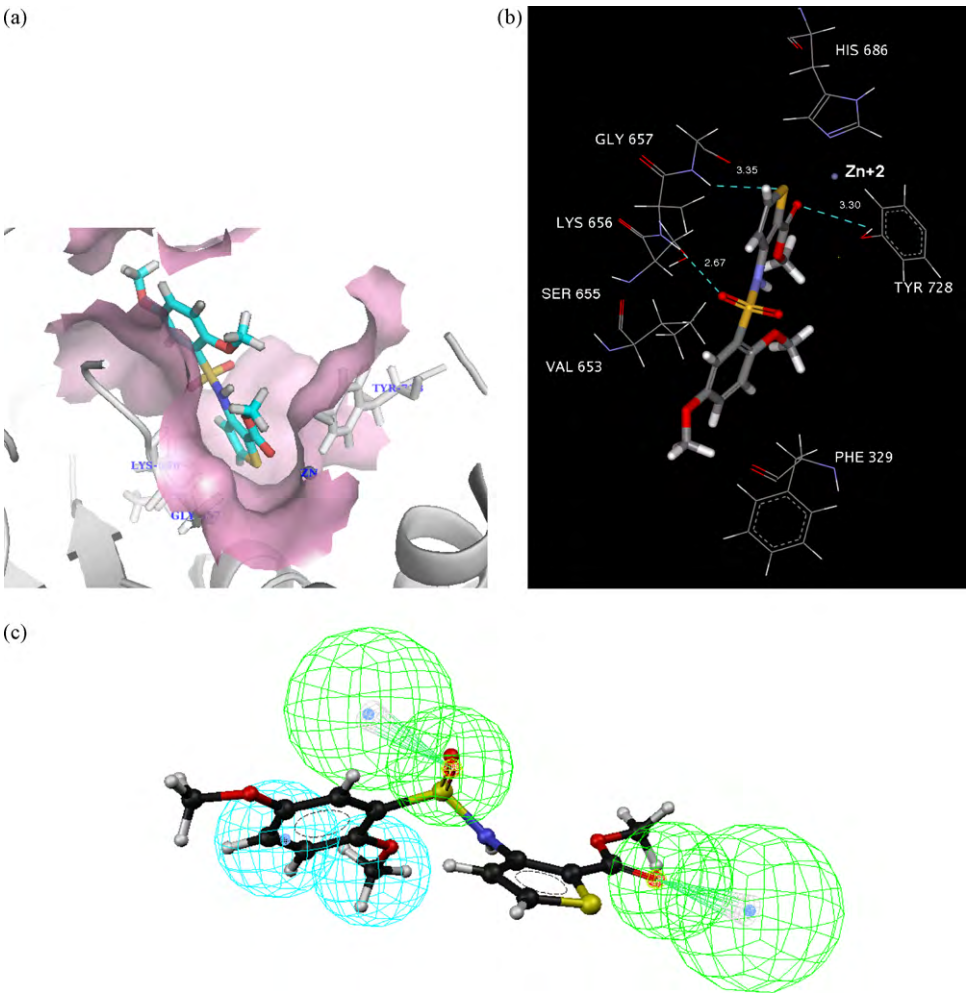

Fig. 9. (a) Docked conformation of the best virtual screening hit (GK02113) in the active site of 1PWU. (b) Representation of interaction between docked conformation of the virtual screening in the active sites of 1PWU. Dashed lines represent hydrogen bonds. (c) Pharmacophore mapping of the virtual screening hit (GK02113) on the best hypothesis model Hypo 1.

model. A screen of our in-house 3D-database of about ~2 M compounds yielded a collection of about 2543 compounds that shared, in some conformation, the same 3D representations of the important functional groups as indicated by Hypo 1. A subset of these structures was created by removing all the molecules that did not satisfy the well-known Lipinski rules, describing properties of drug-like compounds. To increase the probability that a hit is a lead, only molecule that have a fit score between 5.64 and 7.64 were considered for further study. These sets of 120 molecules were docked to Anthrax LF using ligand fit. Docking was performed in order to study the binding orientation and determine favourable interactions within the active site. 17 hits showed high complementarity with the active site of Anthrax LF and can be used as a potential leads to combat anthrax infections. The 2D structures of these 17 virtual screening hits are shown in Scheme 2. The docking interactions and pharmacophore mapping of one of the best hits (GK02113) based on the virtual screening is shown in Fig. 9. Future studies will discuss compound synthesis and their inhibitory activity against Anthrax LF.

5. Conclusion

For the virtual screening of novel and potential compounds against Anthrax LF, quantitative pharmacophore models were generated using structurally diverse compounds, and these models were validated using a test set of 98 compounds. The best model contains two hydrogen bond acceptors (HBA) and two hydrophobic (HY) features and complemented the required ligand-receptor interactions. The docking studies revealed that amino acid Lys656 and Tyr728 are important for ligand binding. Using these pharmacophore and docking models, we have screened a large in-house database for novel inhibitors of Anthrax LF. Virtual screening found 17 hits from the database that showed high complementarity with binding site of the receptor and can be used as potential leads to fight anthrax infections.

Appendix A. Supplementary data

Supplementary data associated with this article can be found, in the online version, at doi:10.1016/j.jmgm.2010.07.002.

References

[1] W.L. Shoop, Y. Xiong, J. Wiltsie, A. Woods, J. Guo, J.V. Pivnichny, T. Felcetto, B.F. Michael, A. Bansal, R.T. Cummings, B.R. Cunningham, A.M. Friedlander, C.M. Douglas, S.B. Patel, D. Wisniewski, G. Scapin, S.P. Salowe, D.M. Zaller, K.T. Chapman, E.M. Scolnick, D.M. Schmatz, K. Bartizal, M. MacCoss, J.D. Hermes, Anthrax lethal factor inhibition, Proc. Natl. Acad. Sci. 22 (2005) 7958–7963.
[2] T. Bell, Anthrax Cleanup Processing inside Hamilton Postal Facility, Associated Press, 2003.
[3] D.R. Bienek, L.J. Loomis, R.E. Biagini, The anthrax vaccine: no new tricks for an old dog, Hum. Vaccine 5 (2009) 184–189.

[4] H.B. Golden, L.E. Watson, H. Lal, S.K. Verma, D.M. Foster, S.R. Kuo, A. Sharma, A. Frankel, D.E. Dostal, Anthrax toxin: pathologic effects on the cardiovascular system, Front. Biosci. 14 (2009) 2335–2357.
[5] D.M. Bravata, J.E. Holty, H. Liu, K.M. McDonald, R.A. Olshen, D.K. Owens, Systematic review: a century of inhalational anthrax cases from 1900 to 2005, Ann. Int. Med. 144 (2006) 270–280.
[6] K.E. Beauregard, R.J. Collier, J.A. Swanson, Proteolytic activation of receptor-bound anthrax protective antigen on macrophages promotes its internalization, Cell Microbiol. 3 (2000) 251–258.
[7] K.A. Bradley, J. Mogridge, M. Mourez, R.J. Collier, J.A. Young, Identification of the cellular receptor for anthrax toxin, Nature 414 (2001) 225–229.
[8] S.H. Leppla, Identification of the cellular receptor for anthrax toxin, Proc. Natl. Acad. Sci. 10 (1982) 3162–3166.
[9] M. Mourez, R.S. Kane, J. Mogridge, S. Metallo, P. Deschatelets, B.R. Sellman, G.M. Whitesides, R.J. Collier, Designing a polyvalent inhibitor of anthrax toxin, Nat. Biotechnol. 10 (2001) 958–961.
[10] R.J. Collier, J.A. Young, Anthrax toxin, Annu. Rev. Cell Dev. Biol. 19 (2003) 45–70.
[11] G.J. Rainey, J.A. Young, Antitoxins: novel strategies to target agents of bioterrorism, Nat. Rev. Microbiol. 9 (2004) 721–726.
[12] G.B. Barcellos, R.A. Caceres, W.F. De Azevedo Jr., Structural studies of shikimate dehydrogenase from Bacillus anthracis complexed with cofactor NADP, J. Mol. Model 15 (2009) 147–155.
[13] I. Pauli, R.A. Caceres, W.F. de Azevedo Jr., Molecular modeling and dynamics studies of shikimate kinase from Bacillus anthracis, Bioorg. Med. Chem. 16 (2008) 8098–8108.
[14] GOSTAR (GVK BIO Online Structure Activity Relationship Database), GVK Biosciences Private Limited, S-1, Phase-1, T.I.E. Hyderabad, A.P, India, 2010. Available from: http://www.gostardb.com.
[15] Cerius2 Software, Accelrys package, version 4.11. Available from: www.accelrys.com.
[16] Catalyst Software, Accelrys package, version 4.11. Available from: www.accelrys.com.
[17] B.E. Turk, T.Y. Wong, R. Schwarzenbacher, E.T. Jarrell, S.H. Leppla, R.J. Collier, R.C. Liddington, L.C. Cantley, The structural basis for substrate and inhibitor selectivity of the anthrax lethal factor, Nat. Struct. Mol. Biol. 11 (2004) 60–66.
[18] M.J.S. Dewar, E.G. Zoebisch, E.F. Healy, J.J.P. Stewart, AM1: a new general purpose quantum mechanical model, J. Am. Chem. Soc. 107 (1985) 3902–3909.
[19] J. Sutter, O. Guner, R. Hoffman, H. Li, M. Waldman, Effect of variable weights and tolerances on predictive model generation, in: O.F. Guner (Ed.), Pharmacophore, Perception, Development, and use in Drug Design, International University Line, La Jolla, Calif., 2000, pp. 501–511.
[20] A. Smellie, S.L. Teig, P. Towbin, Poling: promoting conformational variation, J. Comput. Chem. 16 (1995) 171–187.
[21] A. Smellie, S.D. Kahn, S.L. Teig, Analysis of conformational coverage. 1. Validation and estimation of coverage, J. Chem. Inf. Comput. Sci. 35 (1995) 285–294.
[22] A. Smellie, S.D. Kahn, S.L. Teig, Analysis of conformational coverage. 2. Applications of conformational models, J. Chem. Inf. Comput. Sci. 35 (1995) 295–304.
[23] C.M. Venkatachalam, X. Jiang, T. Oldfield, M. Waldman, LigandFit: a novel method for the shape-directed rapid docking of ligands to protein active sites, J. Mol. Graph. Model. 21 (2003) 289–307.